

INVESTIGATION OF FLOW DYNAMICS AND PLASTIC DEFORMATION IN ARC WELDING USING SPH

Raj DAS^{1*} and Paul W. CLEARY¹

¹ CSIRO Mathematical and Information Sciences, Private Bag 33, Clayton, Victoria 3168, AUSTRALIA
*Corresponding author, E-mail address: raj.das@csiro.au

ABSTRACT

An approach for modelling thermo-mechanical responses in a 3D arc welding process is developed using the Smoothed Particle Hydrodynamics (SPH) method. It is demonstrated for a simple arc welding configuration by using full three-dimensional elastoplastic analysis. The flow pattern of the filler material and the resulting plastic strain distribution are analysed. The effect of welding speed on the plastic deformation in the weld pool is studied. This work establishes the capability of SPH as a tool for gaining insight into the material deposition and plastic deformation in arc welding processes.

INTRODUCTION

Welding is one of the most economical and efficient methods for permanently joining metal structures. Molten filler material from welding wire is transferred to the work piece. It solidifies and bonds the parent parts together. The combination of the heat source, from an arc or generated via friction, and the hot filler material locally melts the material around the weld groove (Naidu *et al.*, 2003). Once the molten filler and the surrounding parent metals cool and solidify, all the components are bonded together. The aim is that the strength of the weld should be at least equal to the strength of the original constituents.

There are many forms of welding, including MIG (Metal Inert Gas), TIG (Tungsten Inert Gas), electroslag, plasma arc, and submerged arc, etc. The choice of welding process is determined by the end use and location of the welded structure (Helzer, 2005). Arc welding is a complex process that involves interplay between different physical processes. In many widely used welding processes, such as Gas Metal Arc Welding (GMAW), the metal transfer, solidification, plastic deformation, and temperature distribution play a crucial role in the generation of residual stresses and the strength of the welded joint (Goldak *et al.*, 1986). The residual stresses generated during welding may have several harmful effects, such as a decrease in the resistance to cyclic loads and corrosion in hostile environments. These effects have been qualitatively understood for many years, but there is still a lack of quantification and ability to predict their behaviour (Kim *et al.*, 2005, Lindgren, 2006).

Numerical modelling of welding has become increasingly important because of its growing application in capital intensive industries, such as marine, mining, rail, oil and gas, and construction. Rapid fluctuations in temperature and continuous phase change occurring during welding make it difficult to instrument and experimentally measure properties in a weld pool. This makes computational modelling an invaluable tool for determining the dynamics within such systems.

Computational modelling can aid in understanding the underlying mechanisms of welding. It can be used to assess the relative importance of various physical processes and predict how different parameters affect the final mechanical and metallurgical properties of the weld.

A number of computational models have been developed to help understand the interaction of filler material with parent parts (Tekriwal and Mazumder, 1986, Kim and Basu, 1998). This interaction is governed by several inter-connected types of physics, including elastoplastic solid deformation, heat transfer, phase transformation, and fluid flow. The complexity is compounded by additional factors controlling the dynamics in the weld pool, such as electro-magnetic forces, surface tension, and gravity.

Many of the limitations of earlier models can be attributed to the computational frameworks used. The modelling approaches undertaken to date have been largely focused on mesh-based techniques (Lindgren, 2006). Conventional mesh-based techniques, such as the Finite Element Method (FEM) and the Boundary Element Method (BEM), have limitations in simulating welding processes as they have difficulties in modelling high deformation and free surface behaviour encountered in welding. Furthermore, the coupling of various physical processes in a multi-phase complex system often poses difficulties. To overcome these, a mesh-free method called Smoothed Particle Hydrodynamics (SPH) has been applied to modelling arc welding processes in 2D (Das and Cleary, 2007, Das and Cleary, 2008). It was shown that the plastic deformation and heat transfer in a welded joint could be effectively simulated using SPH. However, their simulations considered only a 2D model orthogonal to the welding direction, and as a result did not take into account the variation in thermo-mechanical responses in the direction of welding. Here we extend this work and apply SPH to a fully 3D arc welding setup, incorporating the variation of the properties of the weld along the welding direction.

MODELLING APPROACH

In a weld pool, three phases usually interact with each other: (a) solid phase formed by solidification of the liquid/semi-solid metal, (b) liquid/semi-solid phase material in the weld pool, and (c) gas phase above the weld pool due to plasma and shielding gas. In most applications, the shielding gas does not affect the physics of metal transfer and subsequent solidification in the weld pool, other than by affecting the heat transfer. The gas phase can often be ignored in modelling by incorporating its effects using appropriate thermal boundary conditions. To simplify the modelling effort, many models in the

literature assume the entire domain of analysis as a single phase system (Kou and Sun, 1985, Wang *et al.*, 2003). Kou and Sun (1985) modelled the entire system as a liquid phase with different (temperature dependent) viscosities for the filler and workpiece.

We also consider a simplified single phase modelling approach. Here the opposite approach to that used by Kou and Sun (1985) is adopted, i.e. the entire system consisting of filler and parent materials is modelled as a solid phase. The filler material is modelled as a semi-solid (plastic) material with a very low modulus, and the parent parts are modelled as elastic solids. An elastoplastic analysis is performed using SPH to predict the metal deposition and the interaction of the deposited material with the parent materials.

The yield stress of the material increases with decrease in temperature. Here a linear relationship between yield stress and temperature is used (Goldak and Akhlaghi, 2005), given by:

$$\sigma_y = \sigma_{yr} + C_y(T - T_r) \quad (1)$$

where σ_y is the yield stress of the material at temperature T , T_r is a reference temperature, σ_{yr} is the yield stress at temperature T_r , and C_y is a material coefficient. For this problem, we used $T_r = 300$ K, $\sigma_{yr} = 55.2$ MPa, and $C_y = -0.086$ MPa/K.

The basic SPH equations used for fluid flow modelling are given in Cleary *et al.* (2007). A variant of this SPH method was developed by Cleary *et al.* (2006) for simulation of forging and extrusion. In this work, we extend the same SPH formulation for modelling a 3D arc welding process.

SIMULATION CONFIGURATION

We consider a three-dimensional groove weld, which is commonly used for joining two parts edge-to-edge. It is used in T joints, corner joints, and for other complex joints, such as joints between flat and curved surfaces. After deposition into the groove, the filler material subsequently fuses with the parent materials to form the welded joint. Figure 1 shows the geometry of the weld groove and the workpiece (parent materials). We model a typical groove with depth $d = 32$ mm, plate thickness $h = 64$ mm, plate length $l = 100$ mm, and groove angle $\theta = 30^\circ$. The faces of the weld groove from where the welding starts and finishes are termed as the ‘front’ and ‘rear’ ends, respectively (indicated in Figure 1). Two plates are used at the front and rear ends of the weld groove to prevent the filler material from flowing out of the groove. The parent plates are held fixed during welding by clamps around the top, bottom and two sides. Both filler material and workpiece are made from aluminium alloy (A6061) with density, bulk modulus, and shear modulus of 2700 Kg/m³, 70 GPa, and 27 GPa, respectively. The yield stress and hardening modulus are 55.2 and 167 MPa, respectively. The sound speed based on the material properties was 5,092 m/s. The filler rod was initially at 927 C and the workpiece was at room temperature (27 C). The filler rod is moved from front end to rear end with a speed of 0.10 m/s. The filler material flows from top into the V-shaped weld groove under gravity. The planes parallel and orthogonal to the welding direction are termed as the ‘longitudinal’ and ‘transverse’ planes, respectively. The workpiece and filler are discretised into SPH particles with a 3 mm spacing giving a total of 65,648 particles in these three-dimensional simulations.

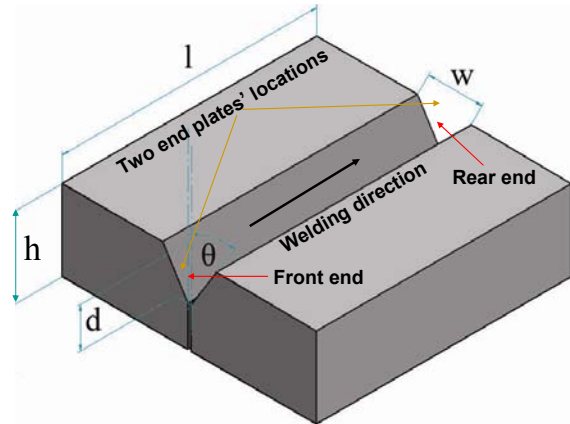


Figure 1: Schematic of a 3D arc welding setup including the V-shaped weld groove (with depth d and width w) and workpiece geometry (with the parent plates on both sides of thickness h).

FLOW DYNAMICS AND PLASTIC DEFORMATION DURING FILLER DEPOSITION

Plastic deformation plays an important role in most welding processes, as emphasised by Bondar and Ogolikhin (1988), Abramov (1986), and Bingert and Fonda (2004). The degree of plastic deformation controls the resultant phase and microstructure, and influences important mechanical properties of welded joints, such as strength, toughness, and corrosion resistance (Kwietniewski *et al.*, 2006).

Figure 2 shows the filler material as it flows under gravity into the weld pool. The left and right columns are coloured by velocity and plastic strain, respectively. For the velocity, the colour variation (blue-red) corresponds to a velocity range of 0.0 to 2.0 m/s, and for plastic strain, it is 0.0 to 10.0. The front and rear end plates (locations shown in Figure 1) are not shown.

Figure 2a shows the filler material flowing in the welding direction at 180 ms. The material in the middle of the weld pool has a uniform velocity (the amber material in the groove). As it approaches the rear plate, it slows down. Some of the material flows reverse to the direction of welding to fill the gap between the filler rod and the front end plate. This material flow is restricted by the front end plate, which diverts the flow upwards. High deformation during this upward flow produces high plastic strains at the front end of the weld groove.

Figure 2b shows the filler material after it strikes the rear end plate. This obstructs the forward motion and deflects the material upwards along the rear plate. The material at the bottom of the weld pool is deformed due to the pressure exerted by the material at the top. The material at the bottom flows over a longer distance than that at the top, leading to a highly deformed layer (called the ‘plastic layer’) at the bottom of the weld pool.

Figure 2c shows the metal flow at 260 ms when the filler rod has advanced one-quarter of the way along the weld pool length. The material deposited has filled almost half of the weld groove. The flow velocity in the middle of the weld pool is higher than that at the rear end. The high plastic strain layer (red) has become thicker both at the bottom of the weld pool and the rear end plate. This layer is fairly uniform in thickness along the welding direction.

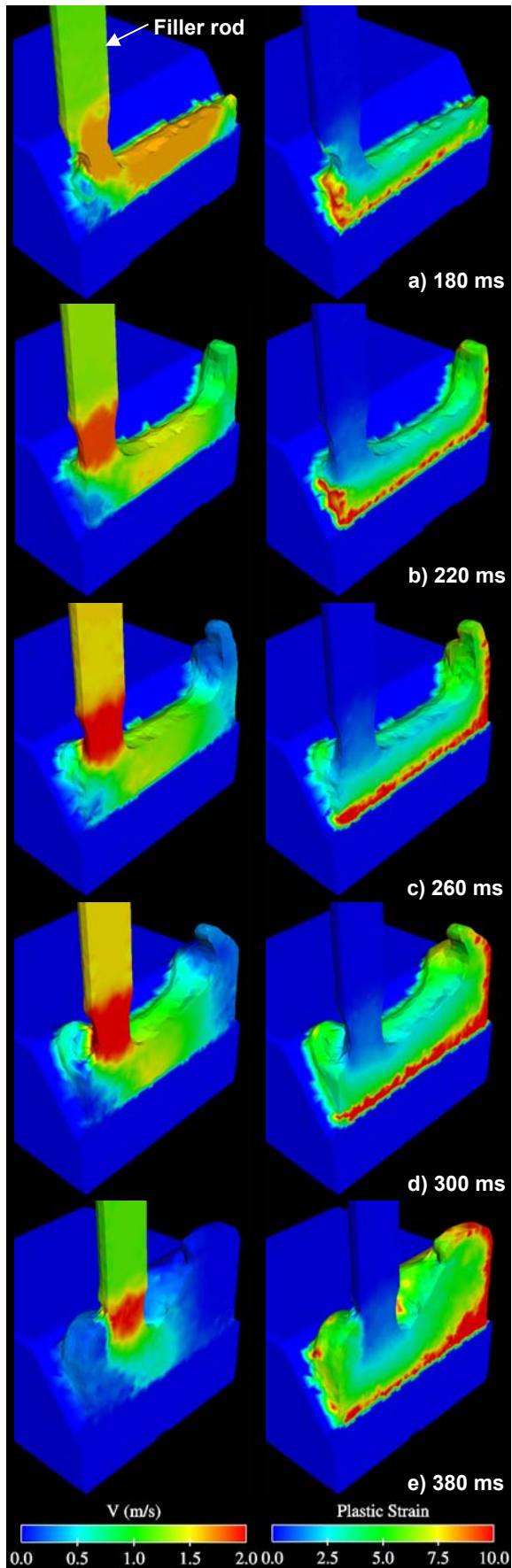


Figure 2: Flow of filler material into the weld groove and the development of plastic strain (sectional views coloured (left) by velocity and (right) by plastic strain).

Figure 2d shows the flow pattern when the weld pool is nearly 80% full. As additional filler material is added, the existing material is pressed towards the ends. This produces high plastic deformation at the bottom and rear end of the weld pool. As a result, gradual thickening of the bottom plastic layer occurs along the welding direction. The high plastic strain layer at the rear end plate is less thick. After flowing upwards over the rear end plate, the material flows backwards into the weld pool, creating a recirculation zone.

Figure 2e shows that as the rear end of the weld groove is nearly filled, the material beneath the filler rod starts flowing reverse to the direction of welding (towards the front end). This pushes the material at the front end upwards. It then flows backwards and re-enters the weld pool. At the rear end, the highly strained plastic layer has grown considerably, because of progressive high deformation and the transport of highly strained material from the front and middle to the rear end. The later reason is supported by the localised variations in plastic strain and thinning of the plastic layer in the front and middle. Some parts of this highly deformed material are also carried up to the top surface, resulting in high plastic strains on the surface.

Throughout the filling process, a pool of stationary material is left behind the filler rod, as it traverses across the weld groove (blue regions behind the filler rod in Figure 2b-e (left)). This material remains trapped between the material beneath the filler rod and the front end plate, and undergoes moderate plastic deformation with plastic strain ranging from 5 to 8.

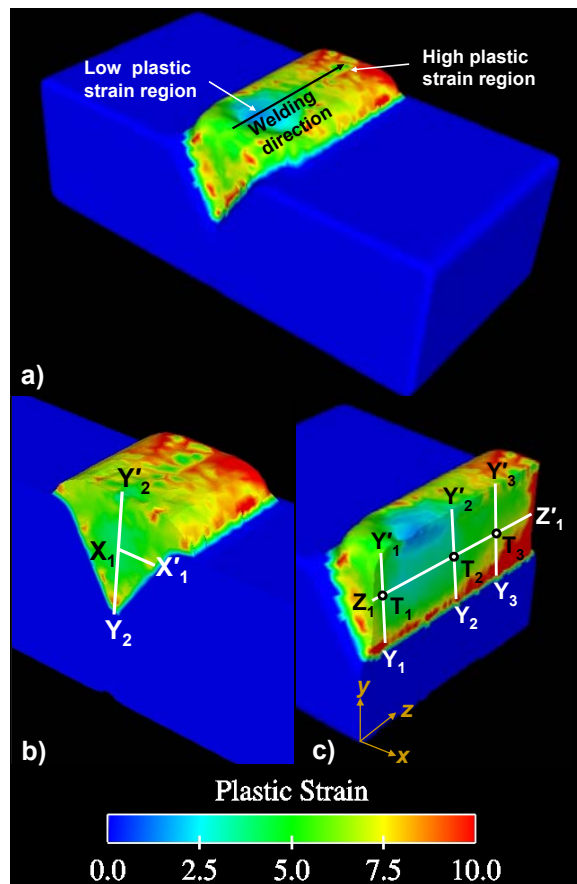


Figure 3: Final plastic strain distribution on (a) the surface of the weld pool, (b) the transverse mid-plane, and (c) the longitudinal mid-plane.

Figure 3 shows the final plastic strain distribution after the weld pool is completely filled. It also shows the line segments used to study the plastic deformation in the weld pool. Figure 3a shows the plastic strain distribution on the weld pool surface. A low strain region near the surface is created at a quarter of the weld pool length (~20 mm) away from the front end. The plastic strain on the surface becomes high (around 10) at the rear end.

Figures 3b and 3c show the plastic strain distributions on the transverse and longitudinal mid-planes, respectively. On the transverse mid-plane, it is fairly uniform in the interior. In contrast, it is higher around the bottom, the free surface, and along the side boundaries (i.e. interfaces with the workpiece). On the longitudinal plane, the plastic strain varies considerably along the direction of welding. The low plastic deformation zone on the weld pool surface (near the front end) penetrates approximately 7 mm into the interior. A layer of highly plastically deformed material is formed at the bottom of the weld pool along the filler-workpiece interface. This plastic layer increases in thickness along the welding direction from the front towards the rear end. The thickening of the plastic layer occurs due to (a) the deformation of the rear end material by the high-speed filler (from behind) against the rear end plate, and (b) the transport of the highly deformed material (along the interface) from the front and middle of the weld groove towards the rear end.

Figure 4 shows the variation of plastic strain in the transverse (x), vertical (y), and longitudinal (z) directions. Figure 4a shows the variation along segment $X_1X'_1$ (shown in Figure 3b) on the transverse plane. The plastic strain gradually increases from 3.9 at the centre up to 4.2 at 6 mm away. It then rises quickly to 5.2 at 8 mm to form a step like structure, where it remains uniform until 10.2 mm from the center. The plastic strain then rises rapidly to 6.7 as the filler-workpiece interface is approached, because of the high deformation of the filler against the workpiece. Figure 4b shows the variation of plastic strain along three vertical lines $Y_1Y'_1$, $Y_2Y'_2$, and $Y_3Y'_3$ (shown in Figure 3c). In all cases the plastic strain is considerably higher at the bottom point of the weld pool, with the values being 14.3, 8.8 and 13.5 at points Y_1 , Y_2 , and Y_3 , respectively. The plastic strain decreases sharply over the first 10 mm, and then remains reasonably uniform until the surface is reached. Here there is a mild increase that represents the skin of material transported from the bottom of the weld pool. Figure 4c shows the plastic strain distribution along the welding direction from the front to rear end through the middle of the deposited material (along $Z_1Z'_1$ in Figure 3c). The plastic strain is 7.4 at the front end. It declines quickly to a minimum of 3.4 at 21 mm along the weld. The plastic strain then increases fairly steadily to 6.9 at 87 mm. Then there is a sharp rise to 12.1 at the rear end. This rapid rise is due to the obstruction of material flow by the rear end plate and the upward sliding of the material along it, which produces high plastic deformation.

Plastic strain influences phase transformation of materials during welding. The non-uniform plastic strain distribution, predicted by SPH, explains the non-homogeneous phase and micro-structure distribution observed in practical welded joints. The difference in the phases between the interior and the peripheral regions of a weld, as observed in reality (Wang *et al.*, 2002), conforms to the similar variation of plastic strain found in this study.

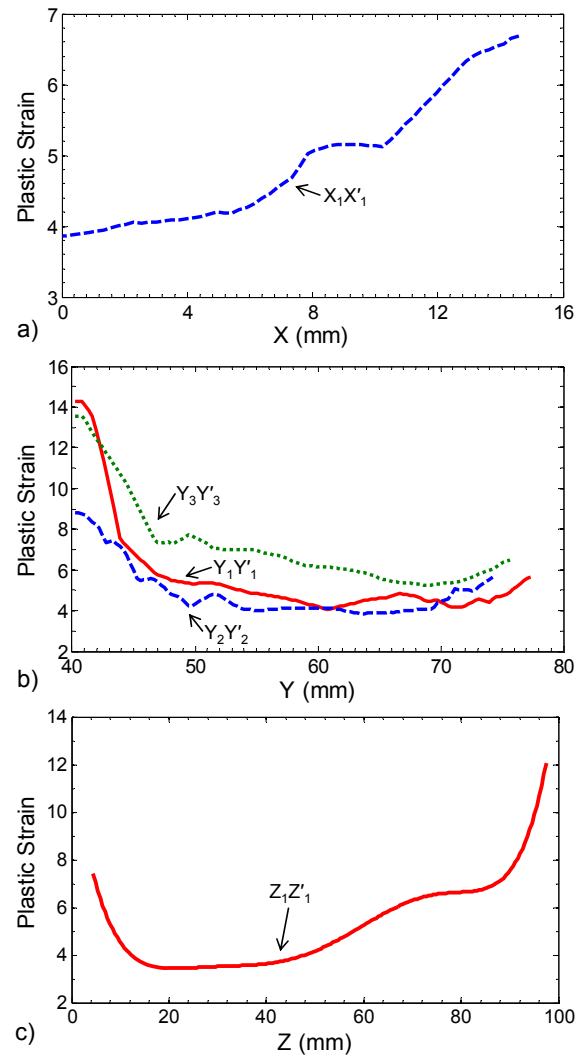


Figure 4: Variation of plastic strain along: a) horizontal line ($X_1X'_1$) on the transverse mid-plane, b) three vertical lines $Y_1Y'_1$, $Y_2Y'_2$, and $Y_3Y'_3$ on the longitudinal mid-plane, and c) along the welding direction $Z_1Z'_1$.

EFFECT OF WELDING SPEED ON PLASTIC STRAIN DISTRIBUTION

Welding speed is one of the most important process parameters. The use of high speed welding reduces the fabrication time, but it may affect the characteristics and mechanical integrity of the joint that is formed.

Figure 5 shows the plastic strain distribution in the weld pool for different welding speeds. Varying the welding speed (v_w) causes a change in the plastic deformation pattern both in the longitudinal and transverse directions of welding. When the welding speed is low ($v_w = 0.10$ m/s), the low plastic strain zone is formed near the front of the weld pool (about 20 mm from the front end as shown in Figure 5a). As the welding speed is increased, the low plastic strain zone moves in the direction of welding towards the rear end. At a speed of 0.15 m/s, it lies midway along the weld pool (Figure 5b). For a higher speed of 0.20 m/s, it moves further away towards the rear end (Figure 5c). The low plastic strain zone on the surface increases in size with increase in the welding speed. An increased speed also leads to higher plastic strains at the front end and lower plastic strains at the rear end.

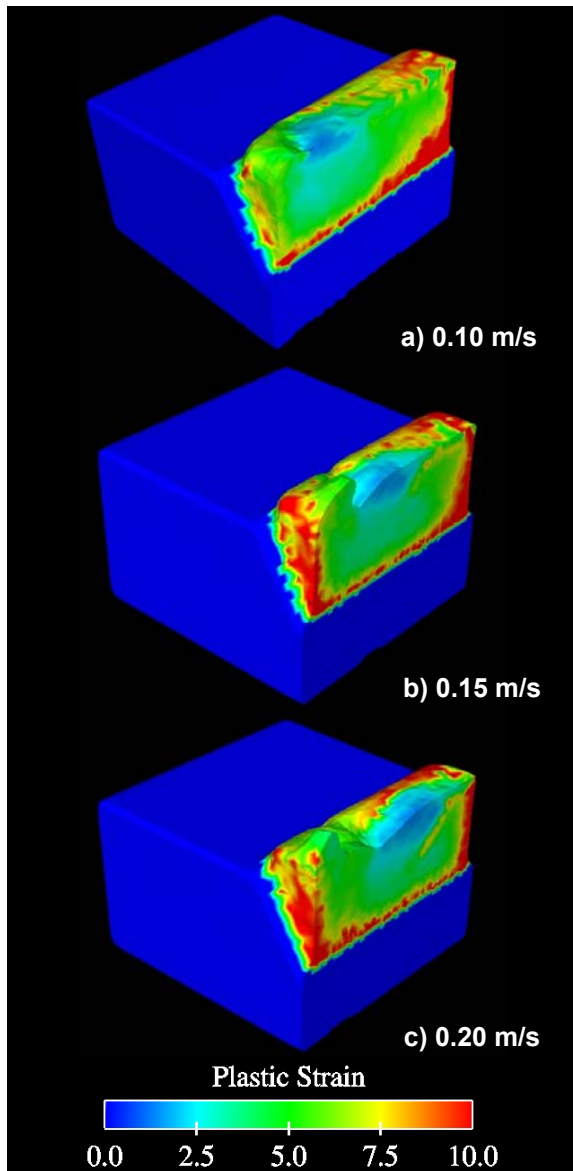


Figure 5: Comparison of the final plastic strain distributions for different welding speeds.

As the filler rod moves faster away from the front end, the filler material flowing reverse to the direction of welding has to travel a longer distance before reaching the front end plate, leading to higher plastic deformation. Conversely, the material flowing along the direction of welding travels a shorter distance before reaching the rear end plate, and undergoes lower plastic deformation. As a result, high speed welding produces higher plastic strains at the front end and lower plastic strains at the rear end, as observed in Figure 5. This shifts the low plastic strain region towards the rear end with increase in speed.

Welding speed also influences the shape of the final weld surface. With an increase in the speed, the weld surface becomes more uneven, with a higher elevation near the front and a depression in front of the low plastic strain (blue) zone. These undulations will affect the fatigue and corrosion properties of the welded joint.

Figure 6 shows the variation in plastic strain along the welding direction for different welding speeds. Ideally, a uniform plastic strain across the weld pool is desirable, because this will contribute to homogenous phase and

microstructure distributions. Points M_1 , M_2 , and M_3 correspond to the 'minimum plastic strains' for the three different cases. These points are located in the low (blue) plastic strain zones in Figure 5. The location of the minimum plastic strain moves from the front end towards the rear end, as the speed of the filler rod is increased. For this problem, the plastic strain reaches its minimum values of 3.5, 3.6, and 4.0 at 21, 51, and 78 mm, respectively from the front end (point Z_1) for the three welding speeds. The most important effect of welding speed is on the degree of uniformity of the plastic strain in the weld pool. At a lower speed ($v_w = 0.10$ m/s), the plastic strain remains approximately uniform over a short distance (between 18 and 42 mm) near the front end. With an increased speed of $v_w = 0.15$ m/s, the plastic strain becomes uniform over a longer region, from 22 to 62 mm, with the minimum point occurring in the middle. When the speed is further increased to 0.20 m/s, the plastic strain becomes less uniform. So there exists a critical welding speed that produces the longest near uniform plastically deformed region in the weld pool. This critical speed lies between 0.10 and 0.20 m/s for this problem geometry and material properties. This study shows that controlling the welding speed can assist in producing a more uniform plastic strain distribution, thus improving the mechanical performance of the joints.

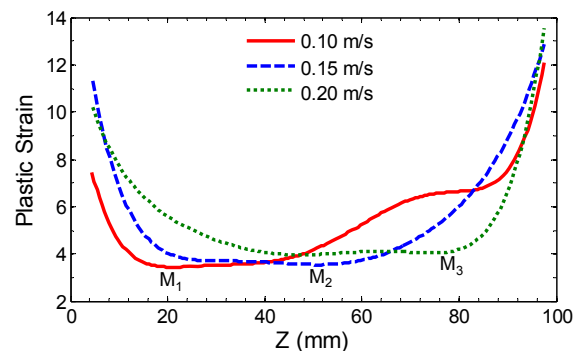


Figure 6: Variation of plastic strain along the welding direction ($Z_1Z'_1$) for different welding speeds.

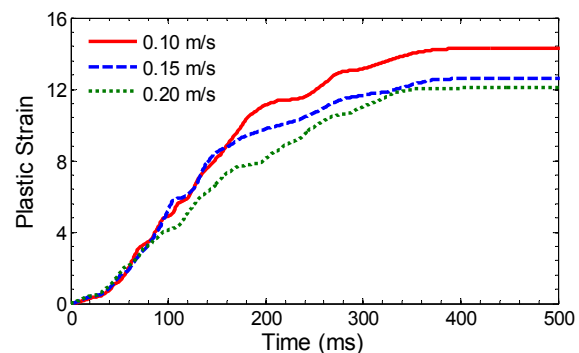


Figure 7: Time variation of the maximum plastic strain for different welding speeds.

Figure 7 shows the variation in the maximum plastic strain during filler material deposition. It increases at nearly the same rate for all cases during the early stage of deposition (up to 100 ms). After the weld groove is filled at 400 ms, the maximum plastic strain becomes constant for each speed. This is because for a completely filled weld groove, the filler material at the bottom (where the

maximum plastic strain occurs) is not deformed any further.

The value of the final maximum plastic strain reduces with an increase in the welding speed. These maximum values corresponding to the three welding speeds are 14.3, 12.6, and 12.1, and they occur at the rear end of the weld. When the speed of the filler rod is greater, the location at which material from the filler rod is added moves closer to the rear end. This material then travels a shorter distance along the welding direction to reach the rear end, and so it undergoes less deformation leading to a lower maximum plastic strain.

CONCLUSION

The application of SPH for modelling a three-dimensional arc welding process has been explored. The solutions demonstrate the key physical processes that occur in typical arc welding. The SPH predictions of plastic deformation and the resulting variation in plastic strain in the weld pool are consistent with behaviour commonly observed in welding.

Arc welding produces a non-uniform plastic deformation in the weld pool with the following characteristics:

- The front and rear ends of the weld pool consist of highly plastically deformed materials.
- High plastic deformation is produced at the interface between the filler and the workpiece.
- The thickness of the plastic layer at the bottom of the weld pool increases from the front to the rear end.
- A skin of high strain material is formed on parts of the free surface of the weld.
- A low plastic strain region is formed in a small area on the surface of the weld pool.

Welding speed is found to considerably affect the plastic strain distribution. With increase in the welding speed, a high plastic strain is developed near the front of the weld pool, and it is reduced at the rear end. Up to a certain critical speed, the plastic strain becomes more uniformly distributed in the middle of the weld pool with increase in the speed. The plastic strain distribution then becomes increasingly non-uniform with further speed increase. So a critical welding speed exists for a given geometry and material of the joint that produces the most uniform plastic strain distribution in the weld pool. This study has demonstrated that welding speed is an important factor that affects the quality of a welded joint. The welding speed can be adjusted so as to enhance the uniformity in the plastic strain, which will contribute to improving the quality of the structural joint. Although a high speed welding may improve the productivity, it may adversely affect the homogeneity of the joints by producing non-uniform plastic deformation.

REFERENCES

ABRAMOV, V. V., (1986), "Plastic deformation of microprojections of bonded surfaces in pressure welding with heating", *Welding Production (English translation of Svarochnoe Proizvodstvo)*, 33 (6), 30-32.

BINGERT, J. F. and FONDA, R. W., (2004), "Severe plastic deformation within a friction-stir weld", *JOM*, 56 (11), 329.

BONDAR, M. P. and OGOLIKHIN, V. M., (1988), "Plastic deformation and bond formation during explosive welding of copper plates", *Combustion, Explosion, and*

Shock Waves (English Translation of Fizika Goreniya i Vzryva), 23, 113-117.

CLEARY, P. W., PRAKASH, M. and HA, J., (2006), "Novel applications of smoothed particle hydrodynamics (SPH) in metal forming", *Journal of Materials Processing Technology*, 177 (1-3), 41-48.

CLEARY, P. W., PRAKASH, M., HA, J., STOKES, N. and SCOTT, C., (2007), "Smooth particle hydrodynamics: status and future potential", *Progress in Computational Fluid Dynamics*, 7 (2-4), 70-90.

DAS, R. and CLEARY, P. W., (2007), "Modelling Plastic Deformation and Thermal Response in Welding using Smoothed Particle Hydrodynamics", In *Proceedings of the 16th Australasian Fluid Mechanics Conference*, 2-7 December Gold Coast, Australia. 253-256.

DAS, R. and CLEARY, P. W., (2008), "On the feasibility of using the mesh-free SPH method for modelling thermo-mechanical responses in arc welding", In *6th International Conference on CFD in Oil & Gas, Metallurgical and Process Industries Trondheim, Norway*.

GOLDAK, J., BIBBY, M., MOORE, J., HOUSE, R. and PATEL, B., (1986), "Computer Modelling of Heat Flow in Welds", *Metall. Trans. B*, 17B, 587-600.

GOLDAK, J. A. and AKHLAGHI, M., (2005), "Computational welding mechanics", New York: Springer.

HELZER, H. B. C. S. C., (2005), "Modern Welding Technology", New Jersey: Pearson Education.

KIM, I. S. and BASU, A., (1998), "Mathematical model of heat transfer and fluid flow in the gas metal arc welding process", *Journal of Materials Processing Technology*, 77 (1-3), 17-24.

KIM, J., IM, S. and KIM, H.-G., (2005), "Numerical implementation of a thermo-elastic-plastic constitutive equation in consideration of transformation plasticity in welding", *Int. Journal of Plasticity*, 21 (7), 1383-1408.

KOU, S. and SUN, D. K., (1985), "Fluid flow and weld penetration in stationary arc welds", *Metall. Trans. A* 16, 203-13.

KWIETNIEWSKI, C., DOS SANTOS, J. F., DA SILVA, A. A. M., PEREIRA, L., STROHAECKER, T. R. and REGULY, A., (2006), "Effect of plastic deformation on the toughness behaviour of radial friction welds in Ti-6Al-4V-0.1Ru titanium alloy", *Materials Science and Engineering A*, 417 (1-2), 49-55.

LINDGREN, L. E., (2006), "Numerical modelling of welding", *Computer Methods in Applied Mechanics and Engineering*, 195 (48-49), 6710-6736.

NAIDU, D. S., OZCELIK, S. and MOORE, K. L., (2003), "Modeling, Sensing and Control of Gas Metal Arc Welding". Elsevier Ltd. .

TEKRIWAL, P. and MAZUMDER, J., (1986), "Finite element modeling of arc welding processes", *Gatlinburg, TN, USA*. 71-80. ASM Int, New York, NY, USA.

WANG, F., HOU, W. K., HU, S. J., KANNATEY-ASIBU, E., SCHULTZ, W. W. and WANG, P. C., (2003), "Modelling and analysis of metal transfer in gas metal arc welding", *Journal of Physics D: Applied Physics*, 36 (9), 1143-1152.

WANG, Y., TSAI, H. L., MARIN, S. P. and WANG, P. C., (2002), "Modeling heat and mass transfer and fluid flow in three-dimensional gas metal arc welding", *New Orleans, LA, United States*. 385-400. American Society of Mechanical Engineers, New York, NY 10016-5990, United States.